

# CAUSES OF THE APPEARANCE OF STRESSES IN AN ICE CORE

V. S. Zagorodnov

Institute of Geography, The Russian Academy of Sciences  
Moscow, Russia

O. V. Nagornov

Moscow Engineering Physics Institute  
Moscow, Russia

J. J. Kelley and K. L. Stanford

Polar Ice Coring Office, University of Alaska Fairbanks  
Fairbanks, Alaska, USA



**Polar Ice Coring Office**  
**University of Alaska Fairbanks**  
**Fairbanks, Alaska 99775-1710**

PICO  
TR-92-4

April 1992

# CAUSES OF THE APPEARANCE OF STRESSES IN AN ICE CORE

V. S. Zagorodnov<sup>4</sup>  
Institute of Geography, the Russian Academy of Sciences,  
29 Staromonetny per., Moscow, 109017, Russia

O. V. Nagornov  
Moscow Engineering Physics Institute,  
31 Kashirskoe Shosse, Moscow, 115409, Russia

J. J. Kelley and K. L. Stanford  
Polar Ice Coring Office, University of Alaska Fairbanks,  
Fairbanks, Alaska 99775-1710, USA

PICO  
TR-92-4

April 1992

<sup>4</sup> V. S. Zagorodnov is presently a visiting research professor at PICO, University of Alaska Fairbanks.

## TABLE OF CONTENTS

|  |     |
|--|-----|
| LIST OF FIGURES .....  | iii |
| ABSTRACT .....   | iv  |
| ACKNOWLEDGMENTS .....  | v   |
| <br>   |     |
| INTRODUCTION .....   | 1   |
| Thermoelastic Stresses in an Ice Core in the Process of Its Formation .....            | 3   |
| Thermoelastic Stresses in an Ice Core Containing Debris .....                          | 9   |
| Stability of an Ice Core as a Pivotal Construction .....                               | 15  |
| Estimation of Thermoelastic Stresses in a Core<br>with Heat Insulation Available ..... | 19  |
| CONCLUSION .....   | 23  |
| REFERENCES .....   | 26  |
| LIST OF SYMBOLS .....  | 27  |

## LIST OF FIGURES

|            |  |    |
|------------|--|----|
| Figure 1.  | Vertical thin section of an ice core segment at a depth of 359 m obtained at Mizuho Station (Antarctica) with a thermal drill in 1983. ....  | 2  |
| Figure 2.  | Main elements of an ice core: $T_w$ – melt point of ice; $T_i$ – temperature of surrounding ice. ....  | 4  |
| Figure 3.  | Temperature distribution in an ice core: a, b and c – height of drill head = 5, 10 and 50 mm, respectively; 1, 2 and 3 – speed of drilling = 10, 7 and 5 m/hr, respectively. ....  | 5  |
| Figure 4.  | Thermoelastic stresses in an ice core: $\sigma_r$ – radial stress; $\sigma_\phi$ – azimuthal stress; $\sigma_z$ – longitudinal stress; $T_i$ – temperature of ice; h – height of drill head; 1, 2 and 3 – drilling speed = 10, 7 and 5 m/hr, respectively. ....  | 8  |
| Figure 5.  | Thermal diffusivity of a mixture of ice and debris: $\chi_i$ – thermal diffusivity of ice; $\chi_m$ – thermal diffusivity of mixture; m – volume concentration of debris. ....   | 11 |
| Figure 6.  | Temperature distribution in an ice core with debris: 1, 2 and 3 – volume concentration of debris = 0, 0.2 and 0.8, respectively; v – drilling rate. ....   | 11 |
| Figure 7.  | Elastic modulus (1) and volume expansion coefficient (2) of a mixture of ice and debris: $E_i$ – ice elastic modulus; $E_m$ – mixture of elastic modulus; $\alpha_i$ – ice volume expansion coefficient; $\alpha_m$ – mixture expansion coefficient; m – debris volume concentration. ....   | 12 |
| Figure 8.  | Azimuthal (a) and radial (b) stresses in ice around debris: 1 – m = 0.2; 2 – m = 0.02. ....  | 16 |
| Figure 9.  | Temperature distribution in an ice core after it has been extracted from the borehole bottom to the glacier surface: $T_b$ – temperature of ice at the glacier bottom; $T_s$ – temperature of ice at the glacier surface; $V_r$ – raising rate of ice core in the borehole; 1 and 2 – ice core with and without thermoinsulation, respectively. .... | 21 |
| Figure 10. | Thermoelastic stresses in an ice core caused by its extraction from a borehole: a – ice core without thermoinsulation; b – thickness of thermoinsulation layer = 5 mm. ....  | 22 |

## ABSTRACT

To improve the quality of an ice core, it is necessary to investigate the probable causes of its stability loss. In this paper, we mainly study the effects accompanying thermal drilling, thermoelastic stresses. The influence of solid inclusions in ice, such as debris or rock fragments at the bottom of the glacier, on thermoelastic stresses is also presented.

A number of questions under consideration relate to both thermal and mechanical drilling. These are the stability of an ice core as a pivotal construction and the estimation of thermoelastic stresses in an ice core under its raising on glacier surface.

## ACKNOWLEDGMENTS

The authors are thankful to their colleagues from PICO and the faculty members of the University of Alaska Fairbanks for their cooperation in the development of new ice drilling technology. Also appreciated is financial support from the National Science Foundation that allows the improvement of antifreeze-thermodrilling technology to continue at the PICO facility at the University of Alaska Fairbanks with the participation of the authors. The assistance of the Institute of Marine Science Publications Office personnel with the editing and preparation of this manuscript for publication is also gratefully acknowledged.

## INTRODUCTION

The extraction of an ice core during the process of deep drilling glaciers is accompanied by a number of effects resulting from the disturbance of its solidity. Micro- and macrocracks can be observed in the core and sometimes only small pieces of shattered ice core are taken from a drilling machine. These effects complicate the study of the isotope and chemical composition of the ice and its physical properties.

To reduce the distortion of the natural properties of an ice core during extraction, it is necessary to understand the behavior of ice subjected to the influence of both thermal and mechanical fields. Thermal equations of state of ice I, water and their mixture under high pressures in a wide range of temperatures have been investigated (Nagornov and Chizhov, 1990). At more temperate pressures, the strength of the ice determines its state. However, there are no quantitative dependencies describing the processes of the fracture of ice. Therefore, we can only try to establish the moment and the point in the ice core where the fracture occurs.

It was noted that the quality of an ice core obtained with an electrothermal drill is lower than that of those extracted by using mechanical drills. Particularly strong cracking of ice cores takes place during the thermal drilling of glaciers at a temperature lower than  $-20^{\circ}\text{C}$  (Fig. 1). A qualitative study of the phenomenon of cracking and the identification of a possible way to prevent ice destruction is necessary for the improvement of the thermal drilling procedure. It will also aid in the development of a new thermal drill design to increase ice core quality. In this paper an attempt will be made to compare the analytical description of thermoelastic stresses appearing in a core during thermal drilling, the stability of the ice core as a pivotal construction, and the results of observations of destroyed ice cores recovered from polar and temperate glaciers.

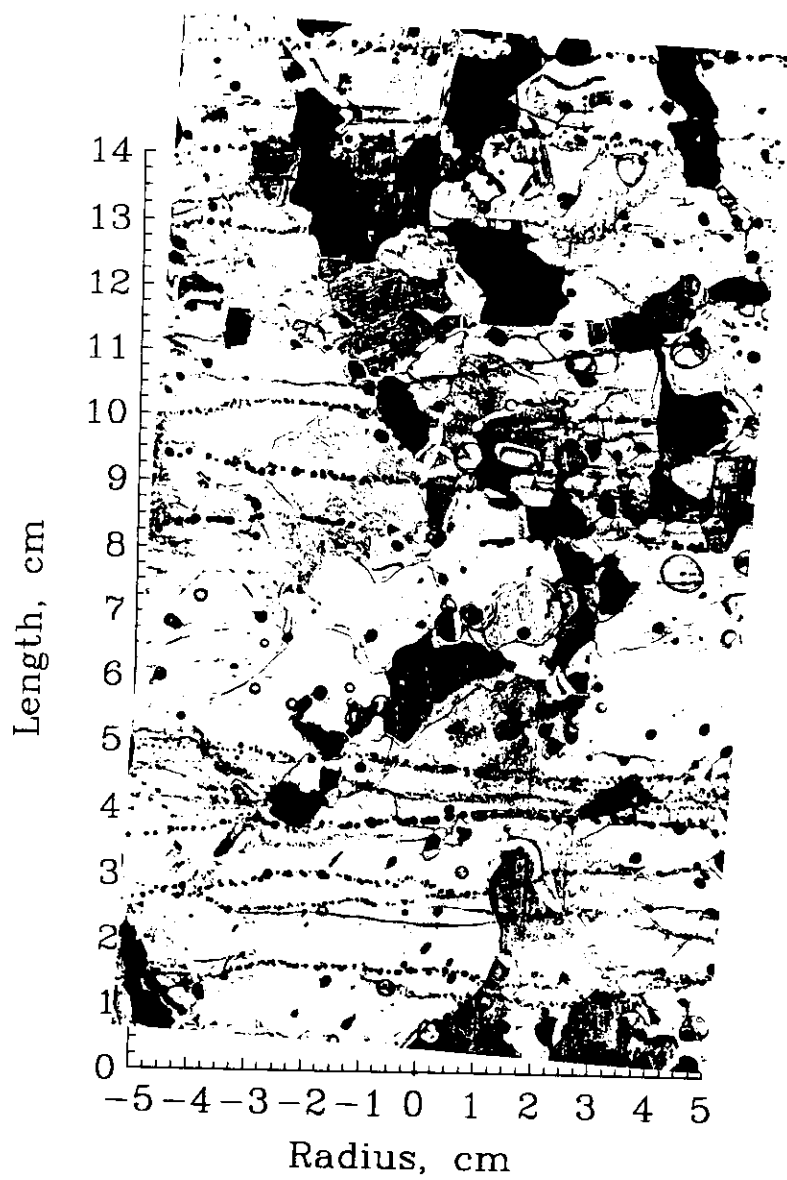


Figure 1. Vertical thin section of an ice core segment at a depth of 359 m obtained at Mizuho Station (Antarctica) with a thermal drill in 1983.



## Thermoelastic Stresses in an Ice Core in the Process of Its Formation

Let us study the field of stresses as they appear in an ice core during its formation under the action of a ring-shaped heater-bit. We shall estimate thermoelastic stresses due to non-uniformity of its heating. Given that stresses are connected with changes of temperature field and added to initial stresses, we shall assume the following: the core is of a cylindrical form and around it there is a liquid interlayer with a temperature  $T_w$ . Under the influence of the heating bit, the ice core will be heated from the side surface (Fig. 2). The depth of the heated zone ( $R-d$ ) is determined by a typical length of heat conduction:  $(4\chi t)^{1/2}$  where  $\chi$  is the thermal diffusivity of ice, and  $t$  is the time of action of a heating source. In our case, the time is determined by the rate of advance of the bit ( $V$ ) and its height ( $h$ ). For example, if  $h = 5$  cm and  $V = 5$  m/hr then  $0 < t < h/V = 36$  sec. The diameter of the ice core is much less than its length. We shall study the central part of the ice core where we can neglect edge effects at the top and the bottom of the ice core. For an estimation of the thermal effects, we assume the core as infinite and limit ourselves to a one-dimensional approximation. Some results of a numerical solution of the differential equation of heat conduction are given in Figure 3 at different heights and speeds of the bit. For time of heating source action, the core does not have time for complete heating along the radius. There is an inner circular region of core where the temperature keeps its initial value and outer heated layer. In a first approximation, the core temperature is considered to be equal to  $T_i$  from  $r=0$  to  $r=d$ , and it is equal to the temperature of ice melting,  $T_w$  at  $d < r < R$ . This simulation is convenient to understanding the phenomenon qualitatively. For quantitative estimations, real distributions of temperature in the ice core will be used.

Thus, if  $u$  is a radial displacement of the core point, then we have the following balance equation:

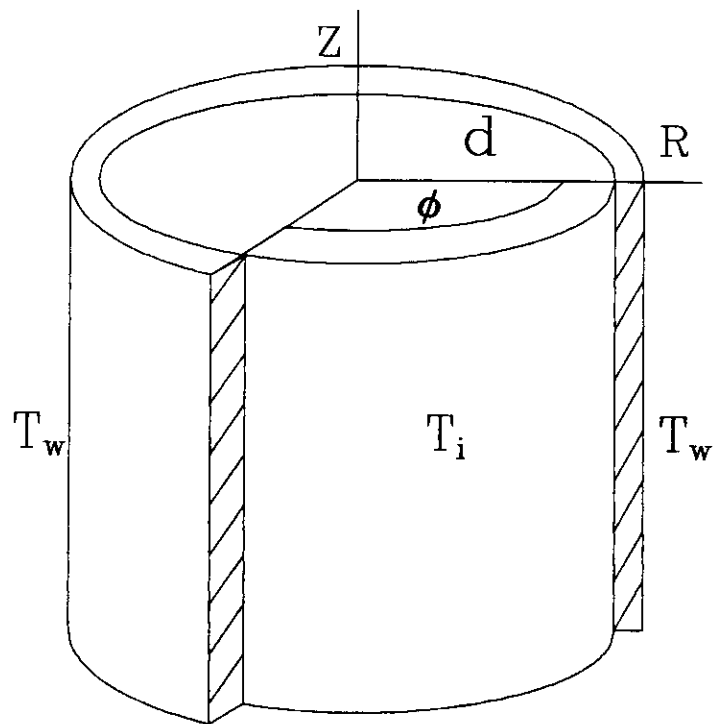


Figure 2. Main elements of an ice core:  
 $T_w$  - melt point of ice;  
 $T_i$  - temperature of surrounding ice.

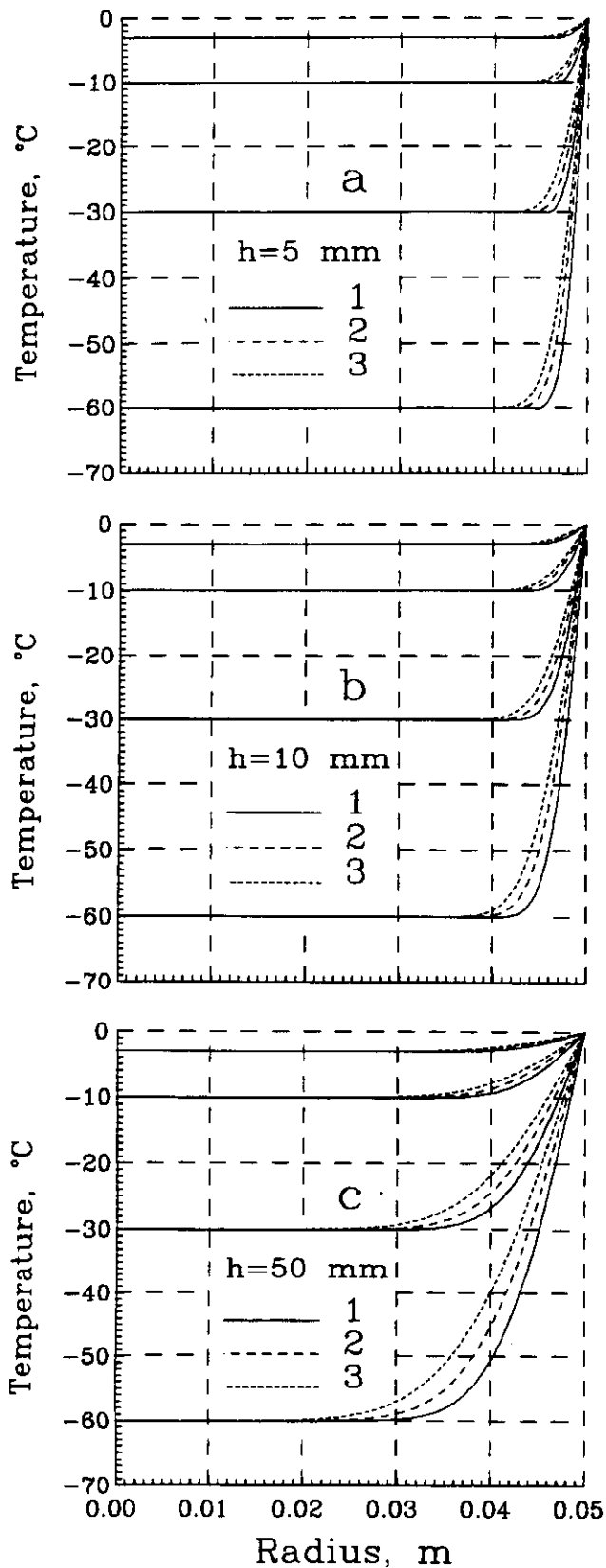


Figure 3. Temperature distribution in an ice core:  
 a, b and c - height of drill head = 5, 10 and 50 mm, respectively;  
 1, 2 and 3 - speed of drilling = 10, 7 and 5 m/hr, respectively.

$$\frac{3(1-\nu)}{1+\nu} \frac{d}{dr} \left( \frac{1}{r} \frac{d}{dr} (ru) \right) = \alpha \frac{dT}{dr} \quad (1.1)$$

Here,  $\nu = 1/3$  is the Poisson coefficient of the ice,  $\alpha = 1.5 \cdot 10^{-4} \text{ K}^{-1}$  is the coefficient of the volume expansion of the ice (Bogorodsky and Gavriilo, 1980), and  $T$  is the temperature of the ice. The speed of change of the thermal field is presumed to be much less than the speed of the longitudinal elastic waves, so the task is quasi-steady. Obviously, the radial stresses at the outer surface of the ice core are  $\sigma_r(R) = 0$ . Here, it is taken into account that the stresses are read off the lithostatic pressure. Then the balance equation is integrated and the following expression for the radial displacement is obtained:

$$u(r) = \alpha(1+\nu)/(1-\nu) \left( \frac{1}{r} \int_0^r T(s) s ds + (1-2\nu)r/R^2 \int_0^R T(s) s ds \right) \quad (1.2)$$

where  $s$  is the integration variable. For the radial stresses we have

$$\sigma_r = E\alpha/(3(1-\nu)) \left( \frac{1}{R^2} \int_0^R T(s) s ds - \frac{1}{r^2} \int_0^r T(s) s ds \right) \quad (1.3)$$

where elastic modulus  $E = (1-\nu^2)\rho c^2$ ,  $\rho$  is ice density, and  $c$  is speed of the longitudinal elastic waves.

The angular and axial components of the stress's tensors  $\sigma_\phi$  and  $\sigma_z$  are equal according to

$$\sigma_\phi = E\alpha/(3(1-\nu)) \left( \frac{1}{r^2} \int_0^r T(s) s ds + \frac{1}{R^2} \int_0^R T(s) s ds - T(r) \right) \quad (1.4)$$

$$\sigma_z = -E\alpha/(3(1-\nu)) \left( 2\nu/R^2 \int_0^R T(s) s ds - T(r) \right) \quad (1.5)$$

Taking into consideration that the temperature distribution is

$$T(r) = \begin{cases} T_i - T_w, & 0 \leq r \leq d \\ 0, & d \leq r \leq R \end{cases} \quad (1.6)$$

we get

$$\sigma_r = \begin{cases} \alpha E(T_w - T_i)(1 - d^2/r^2) / (6(1 - \nu)), & 0 < r < d \\ \alpha E(T_w - T_i)(d^2/r^2 - d^2/R^2) / (6(1 - \nu)), & d < r < R \end{cases} \quad (1.7)$$

$$\sigma_\phi = \begin{cases} \alpha E(T_w - T_i)(1 - d^2/r^2) / (6(1 - \nu)), & 0 < r < d \\ -\alpha E(T_w - T_i)(d^2/r^2 + d^2/R^2) / (6(1 - \nu)), & d < r < R \end{cases} \quad (1.8)$$

$$\sigma_z = \begin{cases} -\alpha E(T_w - T_i)(1 - d^2/r^2) / (3(1 - \nu)), & 0 < r < d \\ -\alpha E(T_w - T_i)(\nu(1 - d^2/r^2) - 1) / (3(1 - \nu)), & d < r < R \end{cases} \quad (1.9)$$

Here, it is taken into account that the temperature is read from the initial ice temperature  $T_i$ . Formulas (1.7) to (1.9) give a qualitative notion of thermoelastic stresses in the ice core and reflect rightly their behavior at the change of heating depth  $(R-d)$ . Distributions of thermoelastic stresses in an ice core are given in Figure 4 at different heights and speeds of the bit with the ice temperature at  $-60^\circ\text{C}$ . These data have been obtained by numerical integration (1.3) to (1.5) after solutions to the corresponding equations of heat conduction were found. The level of thermoelastic stresses is proportional to the difference between the temperature of the ice and the temperature of ice melting. Due to the thermal effects in the heated area  $(R-d)$  of a core, ice expansion in the radial and axial directions takes place. Angular stresses  $(\sigma_\phi)$  in the inner part of an ice core also result in expansion. It follows, also, from formulas (1.8) and (1.9), the greatest stresses occur in the sub-surface layer and are equal to approximately  $6 \cdot 10^5 (T_w - T_i)$  Pa. According to experimental data (Londolt-Bernstein, 1980; Bogorodsky and Gavrilo, 1980), the

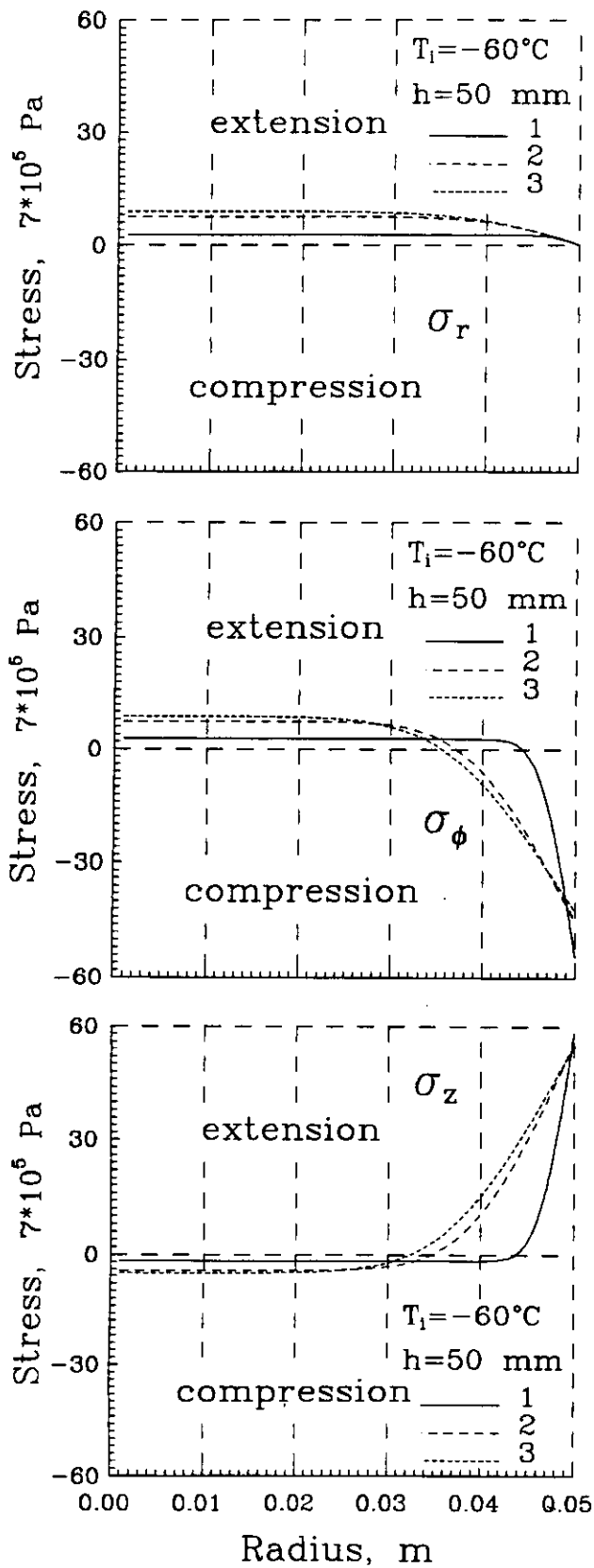


Figure 4. Thermoelastic stresses in an ice core:

- $\sigma_r$  - radial stress;
- $\sigma_\phi$  - azimuthal stress;
- $\sigma_z$  - longitudinal stress;
- $T_i$  - temperature of ice;
- $h$  - height of drill head;
- 1, 2 and 3 - drilling speed = 10, 7 and 5 m/hr, respectively.

strength limit of various types of natural ice is between  $0.2 \cdot 10^6$  to  $3 \cdot 10^6$  Pa. (It should be noted that data about the strength of ice extraction from deep glaciers are absent.) In the process of thermal drilling, some types of ice will crack along the side surface of a core in azimuthal and axial directions at a temperature of only  $-2^\circ\text{C}$ . The cracking of glacial ice due to thermal stresses in the process of thermal drilling begins to manifest itself mainly at temperatures of  $-10$  to  $-15^\circ\text{C}$ .

Volumetric destruction of the central part of a core ( $0 \leq r \leq R-d$ ) is determined by a value of stresses proportional to  $E\alpha/(6(1-\nu))(T_w-T_i)(1-d^2/R^2)$  which manifest themselves in radial, azimuthal and axial directions. With a speed of drilling-melting of 5 m/hr, and core diameter equaling 10 cm, thermal stresses in the central part of the core are equal to approximately  $1.5 \cdot 10^5(T_w-T_i)$  Pa, i.e., four times less than in the sub-surface layer. Indeed, as shown in calculations based on the numerical solution of the heat conduction equation, the ratio of maximal stresses in these parts of the ice core is higher (Fig. 4).

A change in both the height and capacity of the heater will change the time and depth of heating of an ice core. The level of excessive stresses in an ice core is proportional to the ratio of the height of the heater and the speed of drilling-melting.

#### Thermoelastic Stresses in an Ice Core Containing Debris

Physical and mechanical properties of pure ice differ from ice with inclusions (i.e., dirty ice, debris or rock fragments at the bottom of the glacier). To study thermoelastic stresses in an ice core containing inclusion is to suppose there is a homogeneous distribution of inclusions. Its volume concentration is  $m$ . Then the temperature in the core governs the equation of heat conduction and the thermal diffusivity of ice-debris composition ( $\chi_m$ ) then equals (Nikolaevsky, 1984):

$$X_m = \frac{(1-m)\lambda_i + m\lambda_d}{(1-m)\rho_i C_{p i} + m\rho_d C_{p d}} \quad (2.1)$$

where  $\lambda_i$  and  $\lambda_d$  are thermal conductivities,  $\rho_i$  and  $\rho_d$  are densities, and  $C_{p i}$  and  $C_{p d}$  are heat capacities of pure ice and debris, respectively. Properties of inclusions vary widely. For example, if the debris consists of quartzite or basalt, then the thermal diffusivity of the mixture of ice and debris depends on the concentration shown in Figure 5. Distributions of temperature in the core after heating are given in Figure 6. (The initial temperature of the ice was  $-10^\circ\text{C}$ .) In spite of essential changes in the core composition, there are a small variety of temperature distributions.

Compressibility of the two-phase medium  $\beta_m$  can be defined as (Dunin and Nagornov, 1984):

$$\beta_m = (1-m)\beta_i + m\beta_d \quad (2.2)$$

where  $\beta_i$  and  $\beta_d$  are the compressibility of ice and debris, respectively. The elastic modulus  $E_m = (1-\nu_m^2)/\beta_m$  is given in Figure 7. This figure also shows the distribution of the coefficient of the volume expansion of a mixture of ice and debris ( $\alpha_m$ ) dependent upon the concentration of debris. Because the thermoelastic stresses are proportional to the product elastic modulus and to the coefficient of the volume expansion (see (1.3) to (1.5)), thermoelastic stresses will not change significantly if the concentration of debris is increased.

Above, we considered that the core with inclusions is of a homogeneous medium with average properties. However, there is a peculiarity of stresses distributed near the inclusions. Consider spherical inclusions that have an average radius  $a$ . If the concentration of debris is  $m$ , then the medium consists of cells being average radius  $b = a/m^{1/3}$ . Thus, cells have an ice shell with an inner radius  $a$  and an outer radius  $b$ . To calculate micro-thermoelastic stresses in an ice shell is to assume that every cell is



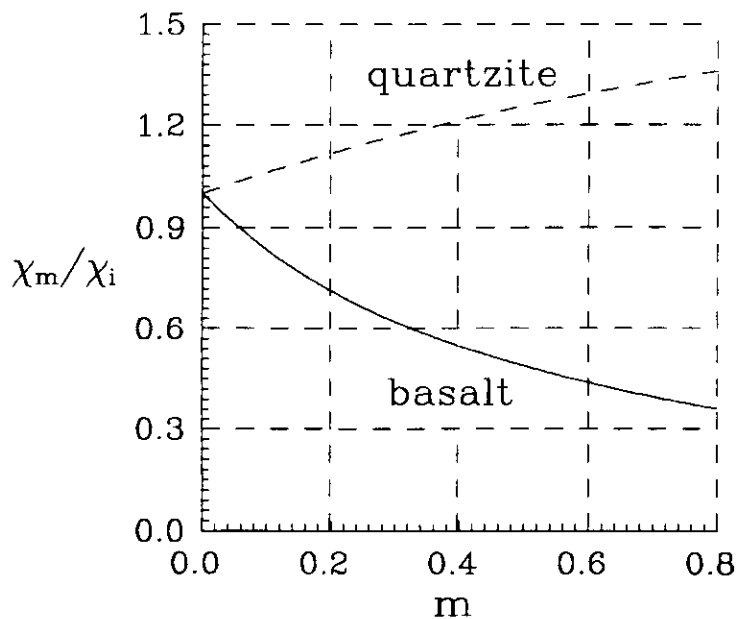


Figure 5. Thermal diffusivity of a mixture of ice and debris:

$\chi_i$  - thermal diffusivity of ice;

$\chi_m$  - thermal diffusivity of mixture;

$m$  - volume concentration of debris.

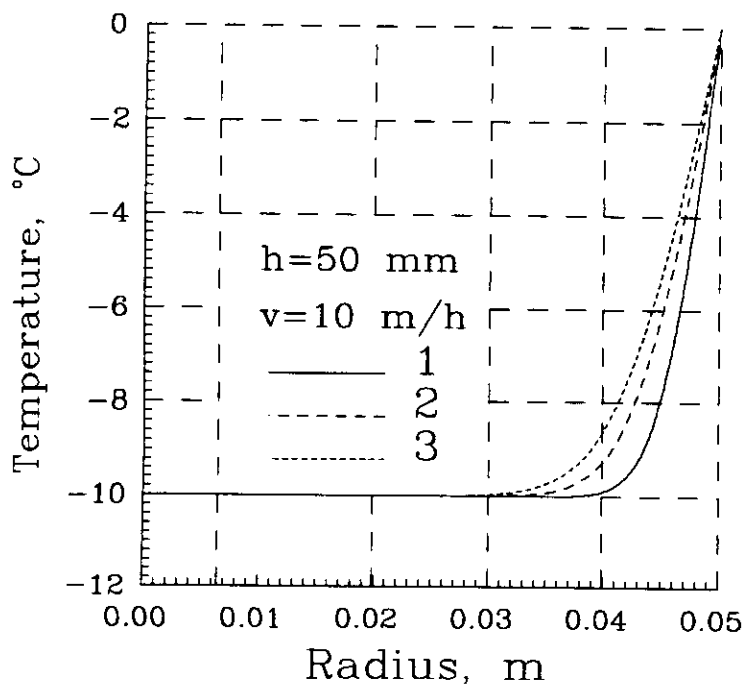
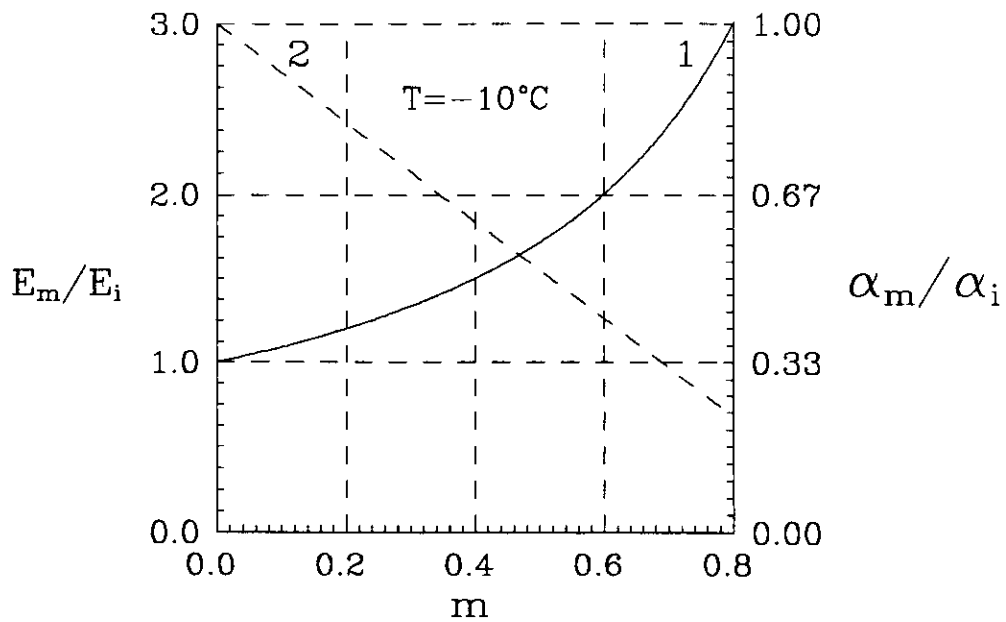


Figure 6. Temperature distribution in an ice core with debris:

1, 2, and 3 - volume concentration of debris = 0, 0.2 and 0.8, respectively;

$v$  - drilling rate.



**Figure 7. Elastic modulus (1) and volume expansion coefficient (2) of a mixture of ice and debris:**

- $E_i$  - ice elastic modulus;
- $E_m$  - mixture of elastic modulus;
- $\alpha_i$  - ice volume expansion coefficient;
- $\alpha_m$  - mixture expansion coefficient;
- $m$  - debris volume concentration.

heating from an initial temperature  $T_i$  to a current temperature  $T_c$ . To describe the distribution of displacements in the cell, we employ the balance equations for each phase

$$\frac{3(1-\nu_d)}{1+\nu_d} \frac{d}{dr} \left( \frac{1}{r^2} \frac{d}{dr} (r^2 u) \right) = \alpha_d \frac{dT}{dr} \quad (2.3)$$

$$\frac{3(1-\nu_i)}{1+\nu_i} \frac{d}{dr} \left( \frac{1}{r^2} \frac{d}{dr} (r^2 u) \right) = \alpha_i \frac{dT}{dr} \quad (2.4)$$

where sub-index d relates to debris and sub-index i relates to ice,  $\alpha$  is the coefficient of temperature expansion, and temperature  $T$  is read from the initial temperature  $T_i$ . At the boundary of debris and ice we have continuity conditions of displacement and radial stresses

$$u(a-0) = u(a+0) \quad (2.5)$$

$$\sigma_r(a-0) = \sigma_r(a+0) \quad (2.6)$$

In the sub-surface layer of an ice core, the average stresses are approximately equal to the lithostatic pressure. Radial stresses at the outer boundary of the cell are

$$\sigma_r(b) = 0 \quad (2.7)$$

because they are read from the initial stresses.

From the last five equations we obtain displacement  $u(r)$ , radial ( $\sigma_r$ ) and azimuthal ( $\sigma_\theta$ ) stresses in ice

$$\sigma_r = \frac{E_i C_1}{1-2\nu_i} - \frac{2E_i C_2}{(1+\nu_i)r^3} - \frac{2E_i \alpha_i}{3(1-\nu_i)r^3} \int_a^r s^2 T(s) ds, \quad (2.8)$$

$$\sigma_{\theta} = \frac{E_i C_1}{1-2\nu_i} - \frac{(2-\nu_i)E_i \alpha_i}{3(1-2\nu_i)(1-\nu_i)r^3} \int_a^r s^2 T(s) ds - \frac{(2-\nu_i)E_i C_2}{(1-2\nu_i)(1+\nu_i)r^3} + \frac{\nu_i E_i \alpha_i T(r)}{3(1-2\nu_i)(1-\nu_i)}; \quad (2.9)$$

$$C_1 = \frac{2(1-2\nu_i)\alpha_i}{3(1-\nu_i)b^3} \int_a^b s^2 T(s) ds + \frac{2(1-2\nu_i)C_2}{(1+\nu_i)b^3}; \quad (2.10)$$

$$C_2 = \left[ \frac{2}{1+\nu_i} \left( \frac{1}{a^3} - \frac{1}{b^3} \right) + \frac{E_d}{E_i(1-2\nu_d)} \left( \frac{2(1-2\nu_i)}{(1+\nu_i)b^3} + \frac{1}{a^3} \right) \right]^{-1} \cdot \left[ \frac{\alpha_d E_d}{E_i(1-2\nu_d)a^3} \int_0^b s^2 T(s) ds + \frac{2\alpha_i}{3(1-\nu_i)b^3} \left( \frac{(1-2\nu_i)E_i}{(1-2\nu_d)E_i} - 1 \right) \int_a^b s^2 T(s) ds \right]. \quad (2.11)$$

If there is uniform heating of the cell, and  $T(r) = T_c - T_i = \Delta T$ , then the formulas are simplified

$$\sigma_r = \frac{E_i C_1}{1-2\nu_i} - \frac{2E_i C_2 b^3}{(1+\nu_i)r^3} - \frac{2E_i \alpha_i \Delta T}{9(1-\nu_i)} \left( 1 - \frac{a^3}{b^3} \right), \quad (2.12)$$

$$\sigma_{\theta} = \frac{E_i C_1}{1-2\nu_i} - \frac{(2-\nu_i)E_i C_2 b^3}{(1-2\nu_i)(1+\nu_i)r^3} - \frac{(2-\nu_i)E_i \alpha_i \Delta T}{9(1-2\nu_i)(1-\nu_i)} \left( 1 - \frac{a^3}{r^3} \right) + \frac{\nu_i E_i \alpha_i \Delta T}{3(1-2\nu_i)(1-\nu_i)}, \quad (2.13)$$

where  $C_1$  and  $C_2$  are defined formulas

$$C_1 = \frac{2(1-2\nu_i)(1-m)\alpha_i \Delta T}{9(1-\nu_i)} + \frac{2(1-2\nu_i)C_2}{1+\nu_i}, \quad (2.14)$$

$$C_2 = \Delta T \left[ \frac{2}{1 + \nu_i} \left( \frac{1}{m} - 1 \right) + \frac{E_d}{E_i(1-2\nu_d)} \left( \frac{2(1-2\nu_i)}{1 + \nu_i} + \frac{1}{m} \right) \right]^{-1} \cdot \left[ \frac{\alpha_d E_d}{3E_i(1-2\nu_d)} + \frac{2(1-m)\alpha_i}{9(1-\nu_i)} \left( \frac{(1-2\nu_i)E_d}{(1-2\nu_d)E_i} - 1 \right) \right]. \quad (2.15)$$

Maximal micro-stresses in the ice shell of a cell are reached at the boundary  $r=a$  and do not depend on the absolute value of  $a$ . It is defined by the properties of the ice, debris and concentration  $m$ . The concentration is bigger and the mean stresses in the ice shell are higher at the same initial radius of inclusions. Distribution of the stresses in the ice shell of a cell are shown in Figure 8 at concentrations  $m=0.02$  and  $m=0.2$ . We have supposed the cell was heating at  $10^\circ\text{C}$ . As it follows from Figure 8, the additional increase of stresses near the inclusions consists of several dozen atmospheres.

### Stability of an Ice Core as a Pivotal Construction

To obtain a monolithic ice core in the form of a cylinder, it is important to identify the conditions under which it is a stable system, i.e., not destroyed under the influence of any small disturbances. Further, possible mechanisms for the loss of ice core stability due to longitudinal pressing forces will be studied.

An equation describing the transversal displacement of a bar under the impact of longitudinal force is as follows:

$$IE \, d^4X/dz^4 - d(PdX/dz)/dz = 0 \quad (3.1)$$

where  $I$  is a modulus of section inertia equal to  $\pi R^4/4$  (Landau and Lifshitz, 1965),  $R$  is the radius of a core cross-section,  $E$  is the elastic modulus (Young's modulus),  $X(z)$  is the deviation of points of elastic line of a core from their initial position,  $z$  is the vertical coordinate along a bar, and  $mgz/l$  is the gravity force of a part of a bar of  $z$

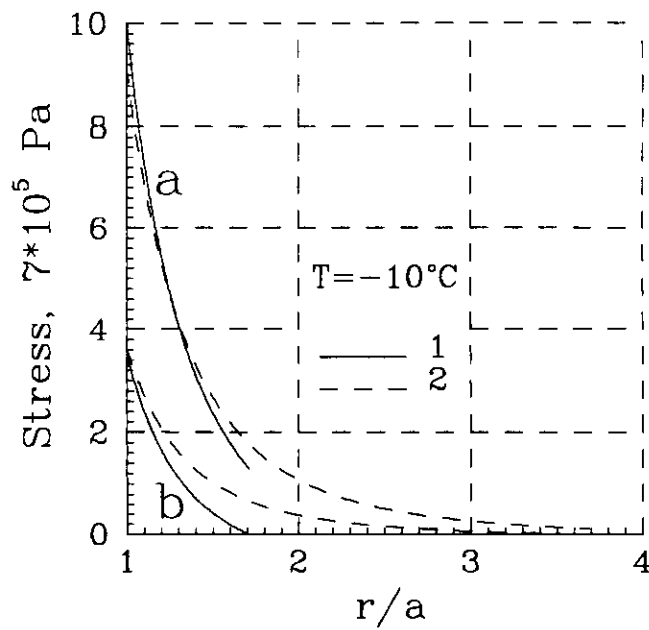


Figure 8. Azimuthal (a) and radial (b) stresses in ice around debris:  
 1 -  $m=0.2$ ;  
 2 -  $m=0.02$ .

height. With the absence of transversal forces, the balance equation of a compressed bar (3.1) has an obvious solution,  $X=0$ , that corresponds to the bar which remains in a straight line. The given solution is stable until the bar length  $l$  is less than the critical length  $l_*$ . If  $l < l_*$ , the rectilinear form of the bar is insensitive to an arbitrary perturbation, so that after this action stops the bar takes a rectilinear form. Accordingly, with  $l > l_*$ , the rectilinear form corresponds to an unstable situation, and with infinite perturbation, a considerable bending will occur, which will result in core cracking. To determine  $l_*$  (either then the trivial solution), all equilibrium solutions of the equation (3.1) should be considered.

As long as the ice core has a cylindrical form, the equation (3.1) is as follows:

$$EI d^4X/dz^4 + d((mgz/l + P)dX/dz)/dz = 0 \quad (3.2)$$

It is possible to take conditions of rigid fixation of the lower end as boundary conditions  $dX/dz(l) = X(l) = 0$ . The upper edge is affected by the longitudinal force  $P$  and  $X(0) = d^2X/dz^2(0) = 0$ . (Both transversal displacement and forces momentums are absent.) From equation (3.2) we have

$$dX^2/dz^2 = \alpha^{1/2} \left[ A J_{1/2} \left( 2/3 (q\alpha^3/(EI))^{1/2} \right) \right] + B N_{1/2} \left[ 2/3 (q\alpha^3/(EI))^{1/2} \right] \quad (3.3)$$

where  $q = mg/l$ ;  $\alpha = l - z + P/q$ ;  $J_{1/2}$  and  $N_{1/2}$  are Bessel's and Neiman's functions, respectively;  $A$  and  $B$  are constants. The critical length  $l_*$  is determined from the boundary conditions and the solution (3.3)

$$J_{1/2} \left[ 2/3 (q/(EI)(l_* + P/q)^3)^{1/2} \right] N_{1/2} \left[ 2/3 (q/(EI)(P/q)^3)^{1/2} \right] - N_{1/2} \left[ 2/3 (q/(EI)(l_* + P/q)^3)^{1/2} \right] J_{1/2} \left[ 2/3 (q/(EI)(P/q)^3)^{1/2} \right] = 0 \quad (3.4)$$

Since the equation (3.4) cannot be solved analytically, let us consider two extreme cases.

Assuming the bar is affected only by its own weight, and the longitudinal load  $P=0$ , then the critical length (Landau and Lifshitz, 1965)  $l = 1.98(EI/mg)^{1/2} = 1.98(c^2R^2/4g)^{1/2}$ . It is obvious from this dependence that the critical length is proportional to  $R^{1/2}$ , and the lower the velocity of elastic waves, the less it is. Estimations on the basis of the known ice parameters (Bogorodsky and Gavriilo, 1980) indicated that the maximum value of  $l_c = 15$  m. While obtaining such an estimation, it was supposed that the moment of inertia  $I$  is determined for a homogeneous, rectilinear, cylindrical core. This definition for the moment of inertia was introduced while calculating the free energy of a homogeneous bar (Landau and Lifshitz, 1965). If the bar is weakened by cracks, its free energy is less and, consequently, the effective radius  $R_f$  included in the formula  $I = \pi R_f^4/4$  is less than the physical radius  $R$ . Hence,

$$l_c = 1.98 (c^2 R_f^4 / (4gR^2)) \quad (3.5)$$

The calculation of free energy of cracked core, its affected section and the influence of the form upon its strength properties are the subjects of a special investigation. It should be noted that since  $R_f$  correlates with  $R^{1/2}$  (see (3.5)), some decrease in the effective section of the core due to its cracking will result in a considerable decrease of  $l_c$ .

If the core weight is neglected ( $mg=0$ ), and we take into consideration the longitudinal force  $P$ , then

$$l_c = (\pi^2 EI / 4P)^{1/2} \quad (3.6)$$

For example, with  $l_c = 15$  m and  $R = 5$  cm, we have  $P = 4 \cdot 10^4$  N.



Obviously, in the process of getting a core, its weight is negligibly small in a borehole filled with liquid. In this case, a homogeneous, rectilinear and cylindrical core can sustain considerable load on its butt-end without destruction. However, while extracting a core, the moment when its own weight affects it, the inevitable happens. In this case, cracks in the sub-surface layer of a core as well as the heterogeneity of the form limit the length of the core extracted from a borehole to the surface.

#### Estimation of Thermoelastic Stresses in a Core with Heat Insulation Available

Consider the case of extracting a core from deep boreholes where the temperature is considerably higher at the bottom than on the surface of a glacier. During extraction, cooling of the sub-surface ice layer takes place and causes thermoelastic stresses similar to the ones considered in the section on formation of thermoelastic stresses. Investigation now turns to the reduction of thermoelastic stresses in an ice core through the use of thermal insulation.

Consider a cylindrical ice core placed into a holder made of heat-insulating material. The temperature  $T(r,t)$  is defined by the following equation:

$$\frac{\partial T}{\partial t} = \chi(r) \left( \frac{\partial^2 T}{\partial r^2} + \frac{1}{r} \frac{\partial T}{\partial r} \right) \quad (4.1)$$

where  $\chi(r) = \chi_i$  ( $0 < r < R_c$ ) is the thermal diffusivity of ice, and  $\chi(r) = \chi_p$  ( $R_c < r < R_s$ ) is the thermal diffusivity of the insulating medium around the core;  $R_c$  and  $R_s$  are the radius of the core and of the shell, respectively. At the boundary of the ice and the heat-insulating shell we have

$$T(t, R_c - 0) = T(t, R_c + 0)$$

$$\lambda_i \frac{\partial T(t, R_c - 0)}{\partial r} = \lambda_p \frac{\partial T(t, R_c + 0)}{\partial r} \quad (4.2)$$

where  $\lambda_i$  and  $\lambda_p$  are the thermal conductivity of ice and the medium surrounding the core, respectively.

At the boundary of the heat-insulating shell, the temperature is

$$T(t, R_s) = T_a \quad (4.3)$$

where  $T_a$  is the temperature of the medium outside the shell. We shall consider typical conditions at the Central Antarctic Ice Sheet (Vostok Station): temperature close to  $-60^\circ\text{C}$  at the glacier surface and about  $-2^\circ\text{C}$  at the glacier bottom. In our case the temperature at the outer boundary of the heat-insulation changes as  $T_a = -2 - 1.074 \cdot 10^{-2} t$  (time  $t$  in seconds). It corresponds to the raising rate of the drill to about 0.75 m/hr.

The initial distribution of the temperature in the core is

$$T(t, r) = T_i, 0 < r < R_c \quad (4.4)$$

The task, (4.1) to (4.4), was solved numerically using a conditionally stable finite-difference scheme of the first order by time and the second order by coordinate. The following parameters were taken next:  $R_c = 5$  cm,  $R_s = 5.5$  cm,  $\chi_i = 1.33 \cdot 10^{-6}$  m<sup>2</sup>/s,  $\chi_p = 0.8 \cdot 10^{-5}$  m<sup>2</sup>/s,  $\lambda_i = 2.3$  j/(m s K),  $\lambda_p = 0.04$  j/(m s K),  $\rho_p = 250$  kg/m<sup>3</sup>,  $T_i = -2^\circ\text{C}$ .  $C_{p i} = 2.09 \cdot 10^3$  j/(kg K) and  $C_{p p} = 2.05 \cdot 10^3$  j/(kg K) are the heat capacity of ice and the insulation, respectively. The chosen properties of insulation are typical for porous materials. The thin heat-insulating layer holds a significant temperature drop. The temperature at the boundary of the core 1.5 hr after being raised is equal to about  $-24^\circ\text{C}$  as the temperature of the ice core without heat-insulation is close to the temperature of the glacier surface (Fig. 9). This means that the level of thermoelastic stresses determined by the change of temperature during core extraction ( $\sigma_1$ ) will be approximately one-third of that without a heat-insulating shell ( $\sigma_0$ ). Distribution of the thermoelastic stresses is shown in Figure 10. It should be noted that stresses

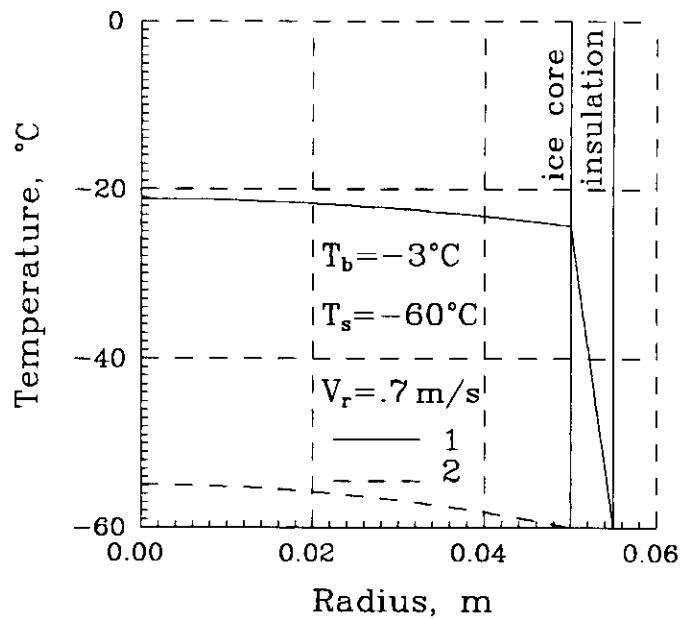


Figure 9. Temperature distribution in an ice core after it has been extracted from the borehole bottom to the glacier surface:

$T_b$  - temperature of ice at the glacier bottom;

$T_s$  - temperature of ice at the glacier surface;

$V_r$  - raising rate of ice core in the borehole.

1 and 2 - ice core with and without thermoinsulation, respectively.

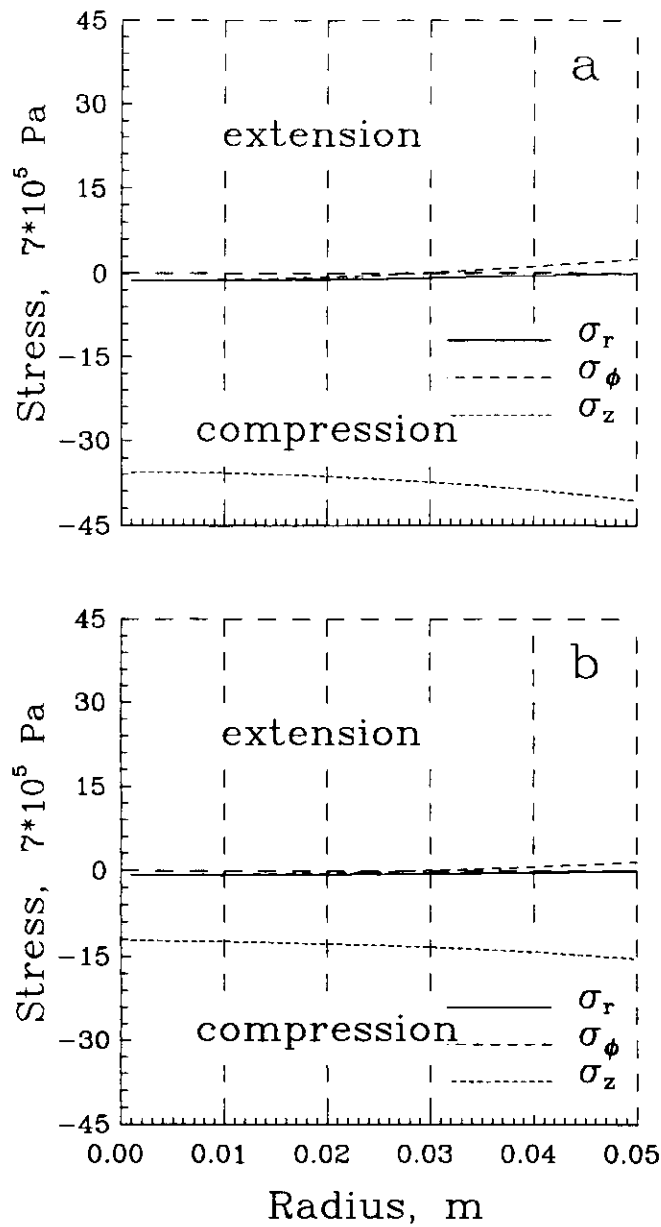


Figure 10. Thermoelastic stresses in an ice core caused by its extraction from a bore hole:

- a - ice core without thermoinsulation;
- b - thickness of thermoinsulation layer = 5 mm.

caused by decompression of ice were not taken into account. There is decompression connected to both elastic unloading of ice by value of corresponding lithostatic pressure and relaxation of inhomogeneities in ice. The last phenomenon is revealing for a relatively long time.

The thermoelastic stresses caused from raising the core are compressible ( $\sigma_r$  and  $\sigma_z$ ), while the elastic stresses in consequence of unloading are extensible. The total stresses in an ice core will depend on thermoelastic stresses (or the difference between temperatures on the surface and at the point of core formation) and the lithostatic pressure (or depth where the core was formed). If this lithostatic pressure  $p_h$  exceeds the maximal value of thermoelastic stresses  $\sigma_0$ , then heat-insulation will not be of any benefit because elastic unloading is compensated by the thermoelastic stresses. Otherwise (if  $\sigma_0 > p_h$ ), heat-insulation will decrease compressible stresses in the ice core.

## CONCLUSION

The investigation showed that during the thermal coring of ice, the greatest stresses occur in the sub-surface layer of a core and are equal to approximately  $6 \cdot 10^5 (T_w - T_i)$  Pa, where  $T_w$  and  $T_i$  are the temperature of ice melting and the temperature of glacier sequence, respectively. In fact, the cracking of the ice core due to thermal stresses during thermal drilling of boreholes filled with antifreeze begins manifesting itself at temperatures of  $-10$  to  $-15^\circ\text{C}$ . When a core loses its solidity, cracks perpendicular to the longitudinal axis, and oblique and scalloped ones up to 0.8 m long appear, and areas of a completely destroyed core consisting of pieces 2 to 3 cm across are also found. It should be noted that along with the evident destruction of a core, distinct microcracks in microsections form in it. These cracks are of concave form running through the core from its surface to approximately its center. The distance between them is typically 2 to 30 mm, and each separate crack occupies 30 to

50% of the cross-section of the core. Thus, the conditions in which the core retains its form are determined. However, its sub-surface layer is contaminated throughout by such cracks. According to Boutron *et al.* (1988), the depth of the penetration of impurities into the core is approximately 2.5 cm. This corresponds well to the estimations given above. Proceeding from the analytical formulas, the level of stresses in a core is proportional to the ratio of the height and the velocity of drilling/melting. To minimize cracking of a core, it is expedient to reduce the height of the thermodrill heater and to increase the velocity of drilling/melting.

In addition to the described cracks, disk-shaped microcracks can form around air bubbles in glacier ice, which appear due to decompression of ice extracted from a depth of several hundred meters. Obviously, besides the above considerations, such disturbances of ice core solidity have a strong effect on its strength properties. However, a theoretical study of the mechanism of air cavity decompression in the ice core is the subject of a special investigation.

The thermal effect generated upon an ice core being extracted from deep boreholes at the temperature differences of up to 30 to 50°C cause thermoelastic stresses sufficient for the appearance of cracks. A heat-insulating shell around a core would considerably decrease these stresses, but expediency of its employment depends also on the correlation of a maximal value of thermoelastic stresses and lithostatic pressure corresponding to the depth where the core was formed. In temperate glaciers, the thermoelastic stresses apparently do not cause cracking of the ice core, and the main action connects to the unloading stresses under the raising of an ice core.

The instability of an ice core as a bar construction, assuming an ideal cylindrical form and the absence of cracks, occurs with lengths of about 15 m. The presence of cracks and the deformation of the form reduce this maximum length. Examples of this, taken during the practice of antifreeze thermal drilling, show that

in a piece of core extracted from a drill 8 cm in diameter and 2 m long, such cracks are observed which are not seen in shorter pieces. The data obtained make it possible to estimate the value of mechanical loads on core butt-ends which do not result in core destruction.

With other conditions being equal, an increase in core diameter will favor the decrease of thermal cracking and will make it possible to extract longer pieces of core from boreholes.

Under the drilling of the transitional zone at the glacier bottom, there can be ice containing rock fragments. There is a concentration of thermoelastic microstresses near these inclusions under thermodrilling. The level of these stresses consists of values approximately  $5 \cdot 10^5 (T_w - T_i)$  Pa at the sub-surface layer that decrease along the radius of the core. As a rule, the temperature at the glacier bottom is close to the melting temperature, so this stress does not essentially effect a stress field.

## REFERENCES

- Bogorodsky, V. V., and V. P. Gavrilov. 1980. Ice. Physical properties. *Modern Methods of Glaciology*. Leningrad, Gydrometeoizdat (in Russian).
- Boutron, C. F., C. C. Patterson and N. I. Barkov. 1988. Assessing the quality thermal drilling antarctic ice cores for trace elements analysis. *In Proceedings of the 3rd International Workshop on Ice Drilling Technology, Grenoble, France*, pp. 182-197.
- Dunin, S. Z., and O. V. Nagornov. 1984. Waves of finite amplitude in soft ground. Translated from Russian. *Izvestiya Akademii Nauk SSSR, MZG*, 5:142-145. Plenum Publishing Corporation, New York, pp. 982-986.
- Landau, L. D., and E. M. Lifshitz. 1965. Elasticity theory. *Moscow. Nauka*. (in Russian).
- Londolt-Bornstein. 1980. Numerical data and functional relations in science and technology. New series. Group IV. Berlin *et al.* Springer.
- Nagornov, O. V., and V. E. Chizhov. 1990. Thermodynamical properties ice, water and their mixture under high pressure. *J. Appl. Mech. Tech. Phys.* (Translated from Russian) 3:41-48.
- Nikolaevsky, V. N. 1984. Mechanics of porous and cracking media. *Moscow. Nedra*, (in Russian).



## LIST OF SYMBOLS

|                   |   |
|-------------------|---|
| A, B              | constant values                                     |
| a                 | radius of inclusions                                |
| b                 | radius of cell                                      |
| c                 | speed of longitudinal elastic waves in ice          |
| $C_1, C_2$        | constant values                                     |
| $C_p$             | heat capacity                                       |
| d                 | radius of unheated area of ice core                 |
| E                 | elastic modulus (Young's modulus)                   |
| g                 | acceleration due to gravity                         |
| h                 | height of thermal bit                               |
| I                 | modulus of section inertia                          |
| $J_{\frac{1}{2}}$ | Bessel's function                                   |
| l                 | core length   |
| m                 | volume concentration of debris (change from 0 to 1) |
| $N_{\frac{1}{2}}$ | Neiman's function                                   |
| P                 | longitudinal force                                  |
| $p_h$             | lithostatic pressure                                |
| q                 | distributive force                                  |
| $R, R_c$          | radius of ice core                                  |
| $R_f$             | effective radius                                    |
| $R_s$             | radius of shell                                     |
| r                 | radial coordinate                                   |
| s                 | integration variable                                |
| t                 | time  |
| T                 | temperature   |
| $T_a$             | temperature of the medium outside core shell        |

|                      |   |
|----------------------|---|
| $T_c$                | current temperature                         |
| $T_w$                | temperature of ice melting                  |
| $u$                  | radial displacement                         |
| $V$                  | speed of advance of thermal bit             |
| $X(z)$               | deviation from core axis                    |
| $z$                  | axial coordinate along core                 |
| $\alpha$             | coefficient of volume expansion             |
| $\beta$              | compressibility                             |
| $\Delta T$           | change of temperature under heating of cell |
| $\nu$                | Poisson coefficient                         |
| $\rho$               | density                                     |
| $\sigma_0, \sigma_1$ | stresses amplitudes                         |
| $\sigma_r$           | radial stresses                             |
| $\sigma_z$           | axial stresses                              |
| $\sigma_\phi$        | angular stresses                            |
| $\sigma_\theta$      | azimuthal stresses                          |
| $\chi$               | thermal diffusivity                         |

Low sub-indexes characterize:

|     |                           |
|-----|---------------------------|
| $d$ | debris                    |
| $i$ | ice                       |
| $m$ | mixture of ice and debris |
| $p$ | insulation shell          |